

Figure 1. (a) Cyclic voltammogram of $[\text{Cp}_4\text{Fe}_4\text{Se}_4]$ (**1**) in 0.1 M TBAB CH_2Cl_2 by a platinum electrode: scan rate 50 mV s^{-1} , $[\mathbf{1}] = 2.5 \times 10^{-4} \text{ M}$. (b) DC polarogram of **1** in 0.1 M TBAB CH_2Cl_2 , $[\mathbf{1}] = 2.5 \times 10^{-4} \text{ M}$.

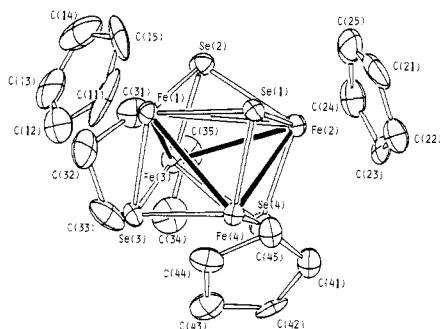


Figure 2. Perspective view of one of the two crystallographically independent trications in $[\text{Cp}_4\text{Fe}_4\text{Se}_4](\text{PF}_6)_3 \cdot \text{CH}_3\text{CN}$. Selected interatomic distances: Fe(1)–Fe(2), 3.358 (4) Å; Fe(3)–Fe(4), 3.353 (3) Å; Fe(1)–Fe(3), 2.839 (3) Å; Fe(2)–Fe(4), 2.802 (4) Å; Fe(2)–Fe(3), 2.933 (4) Å; Fe(1)–Fe(4), 2.777 (3) Å.

there are two kinds of crystallographically independent cationic clusters, their structures are almost the same, with some differences in the orientations of cyclopentadienyl rings. The cubane cluster can be described as a tetracapped tetrahedron with a pseudo- S_4 axis. The four Fe–Se bonds parallel to the axis are shorter (2.260 (3) ~ 2.270 (3) Å) than the others (2.311 (3) ~ 2.350 (3) Å). Four of the six Fe–Fe distances (2.760 (4) ~ 2.974 (4) Å) are shorter than the others (3.353 (3) ~ 3.358 (4) Å) which are perpendicular to the pseudo- S_4 axis. The Fe_4 core of $[\text{Cp}_4\text{Fe}_4\text{Se}_4]^n$ shrinks uniformly with the increase of the charge of the cubane cluster: The average Fe–Fe distances are 3.28, 3.20, 3.11, and 3.02 Å, for the clusters of $n = 0$,³ $2+$,³ and $3+$, respectively. This tendency is due to the stepwise removal of antibonding electrons from the neutral cluster.⁴

$[\text{Cp}_4\text{Fe}_4\text{Se}_4]^n$ is the first example of a cubane cluster on which the species of four successive oxidation states are isolated and crystallographically characterized.

Acknowledgment. The present study was supported by a Grant-in-Aid for Scientific Research, no. 60430011, from the Ministry of Education, Science and Culture.

Supplementary Material Available: X-ray crystallographic data for **4** (13 pages). Ordering information is given on any current masthead page.

(9) **4** was crystallized from acetonitrile–dichloromethane. Crystal data as follows: $\text{C}_{22}\text{H}_{23}\text{F}_{18}\text{Fe}_4\text{NP}_6\text{Se}_4$, FW = 1275.6, monoclinic, space group $P2_1/a$, $a = 20.798$ (4) Å, $b = 17.580$ (3) Å, $c = 19.743$ (3) Å, $\beta = 106.41$ (1)°, $V = 6924.5$ (21) Å³, $Z = 8$; $D_c = 2.45 \text{ g cm}^{-3}$; $\mu(\text{Mo K}\alpha) = 6.47 \text{ mm}^{-1}$. Intensities of 8950 reflections were measured at 13 °C ($2^\circ < 2\theta < 52^\circ$) on a Rigaku AFC-5R diffractometer by using graphite monochromated Mo $K\alpha$ (0.71073 Å) radiation. The structure was solved by the direct method (MULTAN). For 5849 unique reflections ($|F_o| > 3\sigma(F_o)$) the atomic parameters were refined to $R = 0.068$ ($R_w = 0.087$). Details will be reported elsewhere.

Nitrile Hydratase: The First Non-Heme Iron Enzyme with a Typical Low-Spin Fe(III)-Active Center

Yukio Sugiura* and June Kuwahara

Faculty of Pharmaceutical Sciences
Kyoto University, Sakyo-ku, Kyoto 606, Japan

Toru Nagasawa and Hideaki Yamada

Department of Agricultural Chemistry
Kyoto University, Sakyo-ku, Kyoto 606, Japan

Received March 10, 1987

Nitrile hydratase isolated from *Brevibacterium* R312¹ and *Pseudomonas chlororaphis* B23² is a new iron-containing enzyme which catalyzes the hydration of aliphatic nitriles to the corresponding amides: $\text{RCN} + \text{H}_2\text{O} \rightarrow \text{RCONH}_2$. This enzyme is clearly distinguishable from nitrilase that directly converts nitrile to the corresponding acid and ammonia: $\text{RCN} + 2\text{H}_2\text{O} \rightarrow \text{RCOOH} + \text{NH}_3$. The efficient enzymatic transformation of nitrile into amide is useful for bioindustry. No information on the iron center of nitrile hydratase is obtained; however, it is known that no heme iron and no acid-labile sulfur are contained in nitrile hydratase.^{1,2} Herein, we decided to apply electron spin resonance (ESR) spectroscopy to characterize the iron state of the enzyme and found that nitrile hydratase is the first non-heme iron enzyme containing a typical low-spin Fe(III)-active site.

Nitrile hydratase was purified from the crude extract of *Brevibacterium* R312 ($M_w = 85\,000$ and subunit = 3) or *Pseudomonas chlororaphis* B23 ($M_w = 100\,000$ and subunit = 4) according to our previous reports.^{1,2} The crystallized enzymes were homogeneous by polyacrylamide gel electrophoretic and ultracentrifugal analyses. In the enzyme samples, no significant concentrations of transition-metal ions, other than iron, were detected by X-ray fluorescent analysis. Even the dialysis for 48 h at pH 7.5 or pH 6.5 showed no liberations of iron from the enzymes, indicating that the iron atoms are tightly bound to the protein. H_2^{17}O (31.0 atom %) was purchased from B.O.C. Limited, United Kingdom. ESR measurements were run on a JES-FE-3X spectrometer equipped with a liquid nitrogen Dewar flask as a sample holder. The ESR spectra were quantitated by double integration versus a 1 mM copper(II) EDTA standard, with use of the g value corrections of Aasa and Vänngard.³

Figure 1A shows ESR spectrum of native nitrile hydratase isolated from *Brevibacterium* R312 at 77 K. Double integration of the spectrum gave 2.9 ± 0.2 spin per enzyme molecule. The result is consistent with the estimation (2.9 ± 0.1 atoms iron/mol enzyme) of iron analysis by an atomic absorption method, indicating that the enzyme contains one atom iron per subunit. Treatment of a reducing agent such as dithiothreitol to nitrile hydratase resulted in no significant changes of the ESR signals. Of special interest is the fact that the ESR features ($g_{\text{max}} = 2.284$, $g_{\text{mid}} = 2.140$, and $g_{\text{min}} = 1.971$) of the present enzyme are characteristic of rhombic low-spin Fe(III) ($S = 1/2$) type. The iron enzyme is a non-heme iron enzyme but not hemoprotein and ferredoxin because of no existence of iron–porphyrin and acid-labile sulfur.^{1,2} Indeed, the estimated g values differ distinctly from those ($g = 2.05$, 1.94, and 1.88) of a typical iron–sulfur cluster.⁴ In reduced ferredoxin or aconitase, an ESR signal at $g = 1.94$ or 2.01 is attributed to a spin-coupled binuclear or trinuclear iron–sulfur unit.⁵ In an enzymatically active reduced form of purple acid phosphatase, a novel ESR signal centered at

(1) Nagasawa, T.; Ryuno, K.; Yamada, H. *Biochem. Biophys. Res. Commun.* **1986**, *139*, 1305–1312.

(2) Nagasawa, T.; Nanba, H.; Ryuno, K.; Takeuchi, K.; Yamada, H. *Eur. J. Biochem.* **1987**, *162*, 691–698.

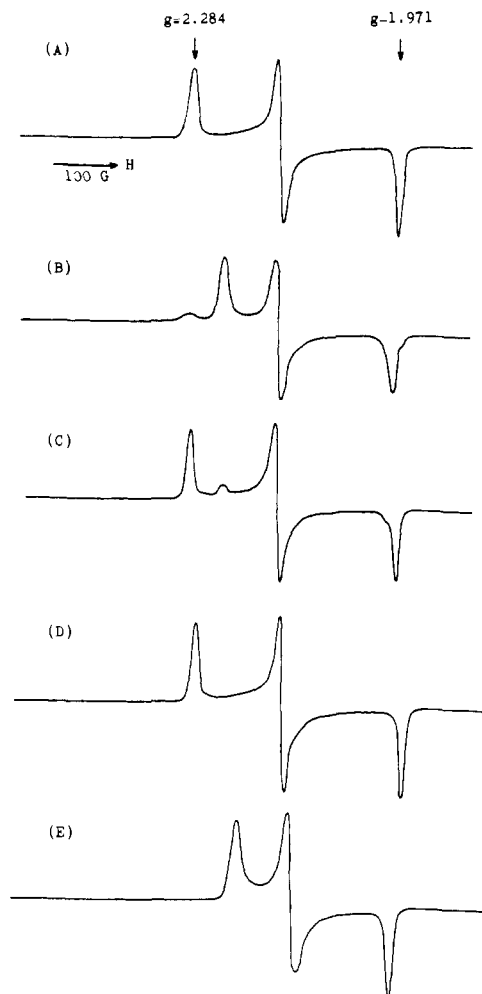
(3) Aasa, R.; Vänngard, T. *J. Magn. Reson.* **1975**, *19*, 308–315.

(4) Beinert, H. In *Iron–Sulfur Proteins III*; Lovenberg, W., Ed.; Academic Press: New York, 1977; pp 61–100.

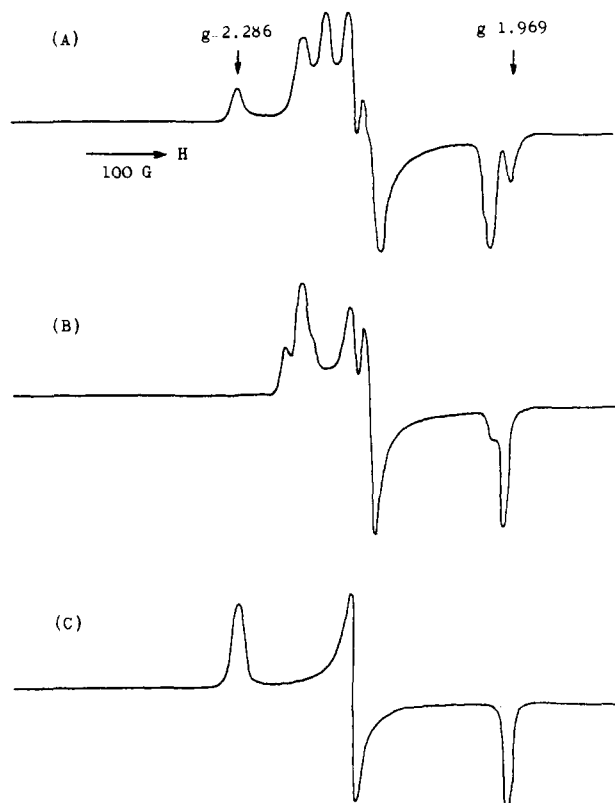
(5) Kent, T. A.; Dreyer, J.-L.; Kennedy, M. C.; Huynh, B. H.; Emptage, M. H.; Beinert, H.; Münck, E. *Proc. Natl. Acad. Sci. U.S.A.* **1982**, *79*, 1096–1100.

Table I. ESR Characteristics of Nitrile Hydratase in Comparison with Low-Spin Iron(III)-Porphyrin and Iron(III)-Bleomycin Complexes

	axial ligtn	g_{\max}	g_{mid}	g_{\min}	$(g_{\max} - g_{\min})$	ref
native R312 enzyme		2.284	2.140	1.971	0.313	
propionitrile-bound R312 enzyme		2.230	2.163	1.982	0.248	
isobutyronitrile-bound R312 enzyme		2.207	2.124	1.984	0.223	this work
mercury-treated native B23 enzyme		2.286	2.141	1.969	0.317	
propionitrile-bound B23 enzyme		2.227	2.161	1.984	0.243	
Fe(PPIXDME)(THF)(SCH ₃ Ph)	O-Fe-S	2.29	2.22	1.97	0.32	
Fe(PPIXDME)(<i>N</i> -MeIm)(SC ₆ H ₄ NO ₂)	N-Fe-S	2.42	2.26	1.91	0.51	8
Fe(PPIXDME)(<i>N</i> -MeIm)(OC ₆ H ₄ NO ₂)	N-Fe-O	2.61	2.21	1.84	0.77	
Fe(PPIXDME)(<i>N</i> -MeIm)(<i>N</i> -MeIm)	N-Fe-N	2.90	2.29	1.57	1.33	
Fe(bleomycin)(SH)	N-Fe-S	2.223	2.148	1.999	0.224	
Fe(bleomycin)(OH)	N-Fe-O	2.431	2.185	1.893	0.538	
Fe(bleomycin)(NH ₃)	N-Fe-N	2.545	2.178	1.837	0.708	7
Fe(bleomycin)(CH ₃ (CH ₂) ₃ NH ₂)	N-Fe-N	2.537	2.179	1.850	0.687	
Fe(bleomycin)((CH ₃) ₃ CNH ₂)	N-Fe-N	2.497	2.181	1.866	0.631	

**Figure 1.** ESR spectra of native nitrile hydratase (0.05 mM) from *Brevibacterium* R312 (A), the enzyme sample obtained immediately after mixing with propionitrile (10 mM) (B), time course (5 min) of the sample B (C), the enzyme plus propionamide (10 mM) (D), and the enzyme plus isobutyronitrile (10 mM) (E) in 0.01 M hepes-KOH buffer (pH 7.2) and 77 K.

$g = 1.77$ is also due to a spin-coupled binuclear iron unit.⁶ So far as we know, therefore, nitrile hydratase is the first non-heme iron enzyme containing a typical low-spin Fe(III) site. A unique example of such a low-spin Fe(III) type appears in the iron(III) complex of bleomycin, a glycopeptide antitumor antibiotic.⁷ Greyish green colored nitrile hydratase from *Brevibacterium* R312 exhibited a visible spectrum with an absorption maximum at 712

**Figure 2.** ESR spectra of native nitrile hydratase (0.03 mM) from *Pseudomonas chlororaphis* B23 (A), the enzyme sample obtained immediately after mixing with propionitrile (10 mM) (B), and the enzyme plus mercury acetate (1 mM) (C) in 0.01 M hepes-KOH buffer (pH 7.2) and 77 K.

nm (ϵ 4200) and no bands (Soret, α , and β) due to porphyrin localized $\pi-\pi^*$ transition in 400–600 nm. A similar spectrum was also noted for nitrile hydratase ($\lambda_{\max} = 720$ nm) isolated from *Pseudomonas chlororaphis* B23. The spectral blue shift from 712 to 690 nm was observed by the addition of propionitrile, suggesting the binding of the substrate to the Fe(III) site of the enzyme. Figure 1B presents the ESR spectrum of propionitrile-bound R312 enzyme. The change in the ESR features of the native enzyme induced by addition of propionitrile ($K_m = 10$ mM), a preferable substrate for this enzyme reaction, converted to the original ESR spectrum after several minutes (Figure 1C). In contrast, the large ESR change brought by addition of isobutyronitrile gave no alterations during several hours (Figure 1E). It is known that isobutyronitrile is barely hydrated in spite of its extraordinary high affinity for the enzyme ($K_i = 5.4 \mu\text{M}$).¹ On the other hand, the addition of propionamide, the enzymatic reaction product, did not truly affect the ESR spectrum of native nitrile hydratase (Figure 1D). Although the native *Pseudomonas chlororaphis* B23 enzyme showed more complicated ESR features than the R312 enzyme, the ESR spectrum of the mercury acetate-treated B23 enzyme

(6) Davis, J.; Averill, B. A. *Proc. Natl. Acad. Sci. U.S.A.* **1982**, *79*, 4623–4627.

(7) Sugiura, Y. *J. Am. Chem. Soc.* **1980**, *102*, 5208–5215.

was remarkably similar to that of the native R312 enzyme (see Figure 2). Double integration of the ESR spectrum of the native B23 enzyme gave 3.8 ± 0.3 spin per enzyme molecule. Nitrile hydratase of *Pseudomonas chlororaphis* B23 contains 4 mol iron/mol enzyme,² and hence its iron environments appear to be unequivalent.

Table I summarizes the ESR parameters of nitrile hydratases in comparison with low-spin iron(III) complexes of porphyrin⁸ and bleomycin.⁷ In general, the g value splitting of low-spin Fe(III) complexes decreases in the order of N-Fe-N > N-Fe-O > N-Fe-S axial ligation modes. The small ($g_{\max} - g_{\min}$) value of nitrile hydratase may suggest that one of the axial ligations is the thiolate donor, probably the cysteine thiol group. Indeed, the ESR features of the present enzyme are considerably close to those of the oxidized cytochrome P-450 state with g values near 2.4, 2.2, and 1.9.⁸ A recent 2.6-Å crystal structure of *Pseudomonas putida* cytochrome P-450 clarified that the heme iron atom is coordinated with the axial sulfur ligand by cysteine residue.⁹ Most of the five-coordinated Fe(III) complexes are not of a low-spin but rather of a high-spin one, and accordingly the most probable other axial ligation of native nitrile hydratase may be water, because of easy replacement by propionitrile or isobutyronitrile. To test whether H₂O is coordinated to the iron(III) site of native R312 enzyme, we have prepared the sample in H₂¹⁷O (31% enriched in ¹⁷O). On substitution of H₂¹⁶O by water enriched in ¹⁷O which has a nuclear spin of 5/2, a 2.5-G broadening (half-peak width) of the $g_{\min} = 1.971$ line was clearly observed. The $g_{\text{mid}} = 2.140$ and $g_{\max} = 2.284$ features were also broadened by 18.2 G (peak to trough) and 22.2 G (half-peak width) from 15.4 and 21.6 G, respectively, as seen for the native enzyme in H₂¹⁶O. The broadenings are attributable to transferred hyperfine interactions, demonstrating that ¹⁷O derived from H₂¹⁷O is coordinated to the iron(III)-active center of nitrile hydratase. On the basis of the broadening of about 3 G at $g = 9.67$ resonance by H₂¹⁶O → H₂¹⁷O replacement, one ligand sphere of the high-spin Fe(III) center in protocatechuate 3,4-dioxygenase is shown to contain water.¹⁰ Similar ESR line broadening by H₂¹⁷O has also been observed for reduced activated aconitase¹¹ and metmyoglobin.¹² In addition, azide ion inhibited the present enzymatic activity and perturbed the ESR spectrum of the native R312 enzyme as follows: $g_{\max} = 2.230$, $g_{\text{mid}} = 2.141$, and $g_{\min} = 1.986$.

In conclusion, the present ESR study reveals that (1) nitrile hydratase is the first non-heme iron enzyme with a typical low-spin Fe(III) coordination environment, (2) axial positions of the iron(III) site in the native enzyme may be occupied by thiolate and aquo groups, and (3) aliphatic nitrile substrates directly bind to the iron(III)-active center by water → substrate replacement. Further characterization of the iron(III)-active site of nitrile hydratase is now underway by Mössbauer, resonance Raman, EXAFS, and X-ray diffraction methods.

Acknowledgment. This study was supported in part by Grant-in-Aid for Special Project Research (61125006 to Y.S.) and Scientific Research B (61490017 to Y.S.) from the Ministry of Education, Science, and Culture, Japan.

Registry No. Fe, 7439-89-6; nitrile hydratase, 82391-37-5; propionitrile, 107-12-0; isobutyronitrile, 78-82-0.

Supplementary Material Available: ESR spectrum of native R312 enzyme in H₂¹⁶O and H₂¹⁷O (Figure S-1) (1 page). Ordering information is given on any current masthead page.

(8) Tang, S. C.; Koch, S.; Papaefthymiou, G. C.; Foner, S.; Frankel, R. B.; Ibers, J. A.; Holm, R. H. *J. Am. Chem. Soc.* **1976**, *98*, 2414-2434.

(9) Poulos, T. L.; Finzel, B. C.; Gunsalus, I. C.; Wagner, G. C.; Kraut, J. *J. Biol. Chem.* **1985**, *260*, 16122-16130.

(10) Lipscomb, J. D. In *Oxygenases and Oxygen Metabolism*; Nozaki, M., Yamamoto, S., Ishimura, Y., Coon, M. J., Ernster, L., Estabrook, R. W., Eds.; Academic Press: New York, 1982; pp 27-38.

(11) Emptage, M. H.; Kent, T. A.; Kennedy, M. C.; Beinert, H.; Münck, E. *Proc. Natl. Acad. Sci. U.S.A.* **1983**, *80*, 4674-4678.

(12) Vuk-Pavlovic, S.; Siderer, Y. *Biochem. Biophys. Res. Commun.* **1977**, *79*, 885-889.

Template-Controlled Oligomerization of Methyl Methacrylate

Ken S. Feldman* and Yoon B. Lee

Department of Chemistry
The Pennsylvania State University
University Park, Pennsylvania 16802

Received April 20, 1987

Many molecules of longstanding interest to organic chemists contain, as part of their structure, a finite segment of repeating units. The challenges posed by the synthesis of these repetitive segments have been addressed to date by an iterative approach: addition of successive "monomers" accompanied by oxidation level adjustments and protection/deprotection steps. While implementation of these strategies can be tedious and is often inefficient, the resultant stereo- and regiochemical control of bond formation has been excellent.¹

Herein, we report our preliminary results concerning a conceptually new strategy, which we term *template-controlled oligomerization*, for the construction of repeating segments within structurally complex molecules. This alternative approach to iterative methodology relies on a linear addition of a predetermined number of monomer units to assemble the desired oligomeric target in a single operation.

Successful execution of this strategy depends upon precise control of the timing of the three stages of an oligomerization process (i.e., initiation, propagation, and termination), since the overall length of the product oligomer will be determined by the number of monomers incorporated into the growing chain during the propagation phase. Therefore, the critical challenge of this approach hinges upon the ability to insert a "stop message" (i.e., termination event) at a predetermined time into an actively polymerizing system.

Our experimental approach utilizes the large rigid spacer² template **1** to fix the positions of an initiating (I) and a terminating (T) functionality for a given polymerization reaction.³ In the ideal experiment, polymerization will occur only within the initiator-terminator gap, and, hence, the length of the oligomeric product will depend solely on template size. A primary obstacle in realizing this ideal template-controlled oligomerization scheme arises from the anticipated competition between desired intramolecular termination and undesired bimolecular termination events. This important issue of the efficiency of intramolecular termination was initially probed via the experiments outlined in eq 1.

The dihydroxy template **2a** was employed in a *macro-lactonization* process that was designed to model the *macro-cyclization* reaction which would constitute intramolecular termination in a polymerizing system. Equimolar quantities of bis acid chloride **3** and template diol **2a** were allowed to react in the presence of dimethylaminopyridine in methylene chloride under high dilution for 18 h leading to the results shown in eq 1.⁴

(1) (a) Katsuki, T.; Lee, A. W. M.; Ma, P.; Martin, V. S.; Masamune, S.; Sharpless, K. B.; Tuddenham, D.; Walker, T. *J. Org. Chem.* **1982**, *47*, 1373. (b) Lipshutz, B. H.; Katsuki, H.; Lew, W. *Tetrahedron Lett.* **1986**, *27*, 4825. (c) Nicolaou, K. C.; Uenishi, J. *J. Chem. Soc., Chem. Commun.* **1982**, 1292. (d) See: Heathcock, C. H. In *Asymmetric Synthesis*, Morrison, J. D., Ed.; Academic Press: Orlando, FL, 1984; Vol. 3, and references cited therein.

(2) Examples of the use of organized structures (including templates) to control the dynamics of a polymerization process can be found in the following: (a) Imprint Polymerization: Wulff, G. In *Polymeric Reagents and Catalysts*; Ford, W. T., Ed.; ACS Symposium Series 308; 1986. (b) Replica Polymerization: Bamford, C. In *Developments in Polymerization*; Haward, R. N., Ed.; Applied Science Publishers, Ltd.; London, 1979; Vol. 2. (c) Polymerization in Organized Media: *Polymerization of Organized Systems*; Elias, H.-G., Ed.; Gordon and Breach Scientific Publishers: New York, 1977.

(3) The templates of general structure **1** were readily prepared from double Diels-Alder addition of anthracene 9-methylcarboxylate to the trans-anti-trans norbornadiene trimer,⁹ followed by functional group manipulation to deliver the appropriate initiator/terminator pairings. The preparation and subsequent manipulations of these species will be detailed in a forthcoming publication.

(4) All new compounds exhibited satisfactory spectral data (¹H NMR, ¹³C NMR, IR, MS, and elemental analysis).